

# Evolution of Primary $\alpha$ Phase Morphology and Mechanical Properties of a Novel High-Strength Titanium Alloy during Heat Treatment

Zhou Wei, Ge Peng, Zhao Yongqing, Xin Shewei, Li Qian, Chen Jun, Zhang Siyuan, Huang Chaowen

Northwest Institute for Nonferrous Metal Research, Xi'an 710016, China

**Abstract:** The evolution of primary  $\alpha$  phase morphology and mechanical properties of a novel high-strength titanium alloy during heat treatment were investigated. The results show that the primary  $\alpha$  phases exhibit a globular growth feature on the basis of the equiaxed  $\alpha$  phases under double solution treatment at air cooling process of  $\alpha/\beta$  zone. But abnormal growth of primary  $\alpha$  grains occurs in the 0.5 °C/min furnace cooling process except that some primary  $\alpha$  remains spherical growth, i.e. the other part of  $\alpha$  grains evolve into similar “fork” shaped dendritic growth rather than keeping nearly spherical growth trend. The novel titanium alloy has attractive combinations of strength and ductility ( $\approx 1300$ MPa of ultimate strength with 10.5% of elongation) owing to the microstructures of equiaxed or thin billet-like primary  $\alpha$  phase and fine needle-like secondary  $\alpha$  phase after  $\alpha/\beta$  solution treatment followed by air cooling plus aging. After  $\alpha/\beta$  solution treatment followed by furnace cooling to low temperature and then aging heat treatment, the new type alloy has an excellent fracture toughness ( $\geq 80$  MPa $\cdot$ m<sup>1/2</sup>), and the elongation and reduction of area remain at about 19% and 45%, respectively, and its corresponding tensile strength is maintained at about 1000 MPa. It can be assumed that the alloy may be a usable structural material.

**Key words:** heat treatment; titanium alloy; primary  $\alpha$  phase; mechanical properties

In recent years, titanium alloys are very attractive for automotive, aerospace and medical industries as structural parts due to their low density and high strength-to-density ratios<sup>[1,2]</sup>. Structural titanium alloys are generally divided into four categories: near  $\alpha$  alloys,  $\alpha+\beta$  alloys,  $\beta$  alloys consisting of metastable and stable  $\beta$  alloys and intermetallics (Ti<sub>3</sub>Al and TiAl based alloys). Among them,  $\beta$  titanium alloys have been widely used in many demanding structural applications due to their excellent strength/toughness combination<sup>[3-6]</sup>. For example, the commercially  $\beta$  titanium alloy Ti-13V-11Cr-3Al was developed to use on the SR-71 “Blackbird” reconnaissance airplane<sup>[7]</sup> and Ti-10V-2Fe-3Al (Ti-10-2-3) was used in landing gear forgings for the Boeing 777 for its improved fatigue performance and weldability<sup>[8]</sup>. However, to obtain such good mechanical behaviour is not easy because the mechanical

properties of these alloys are determined by many factors.

It is well known that microstructure has a significant effect on mechanical behaviour of  $\beta$  titanium alloy<sup>[9,10]</sup>. The  $\beta$  phase may decompose into primary  $\alpha$  phase ( $\alpha_p$ ), secondary  $\alpha$  phase ( $\alpha_s$ ) and/or  $\omega$  particles<sup>[11]</sup> during solution plus aging (STA)<sup>[12]</sup> treatment process for  $\beta$  titanium alloy. The morphology of primary  $\alpha$  phase can affect the ductility, and the size and distribution of fine secondary  $\alpha$  phase particles aged precipitation can affect the strength level<sup>[13]</sup>. Generally, producing an optimum set of properties, for example balancing strength, toughness and ductility is thus expected to control the microstructure parameters including the size, volume fraction, morphology and distribution of both the primary and secondary  $\alpha$  phase.

A novel  $\beta$  titanium alloy which designed by Northwest Institute for Nonferrous Metal Research (NIN) in China contains

Received date: October 26, 2016

Foundation item: National Natural Science Foundation of China (51471136); International Science and Technology Cooperation (2015DFA51430)

Corresponding author: Zhou Wei, Master, Titanium Alloy Research Center, Northwest Institute for Nonferrous Metal Research, Xi'an 710016, P. R. China, Tel: 0086-29-86250729, E-mail: zhouwei2002563@163.com

Copyright © 2017, Northwest Institute for Nonferrous Metal Research. Published by Elsevier BV. All rights reserved.

$\beta$  stabilizing elements Cr, Fe, Mo, W and  $\alpha$  stabilizing element Al, and it has been studied in this paper. The molybdenum equivalent of the novel alloy is about 13 according to the composition and the empirical equation. Its design is to achieve an excellent combination of high strength and high fracture toughness based on the multi-component strengthening. However, as a novel designed alloy, the microstructural features and mechanical properties are not well understood yet. Therefore, the present work is undertaken to understand the relationship between primary  $\alpha$  phase morphology characteristics and tensile properties of the alloy during the  $\alpha/\beta$  solution treatment and subsequent aging, and concurrently, and to reveal how the microstructures of the novel alloy change by heat treatments and how the changes affect the tensile properties.

## 1 Experiment

The ingot of the alloy, about 160 mm in diameter and 300 mm in height, was prepared by triple vacuum arc remelting. The  $\beta$  transus temperature ( $T_\beta$ ) of the material obtained by metallographic technique was  $880 \pm 5^\circ\text{C}$ . The processing of the ingot consisted of primary forging at  $1150^\circ\text{C}$  to break down the as-cast structure, and finish forging at  $830^\circ\text{C}$ . Eventually, a billet with a square cross section of 80 mm was obtained. Fig.1 shows the microstructure of alloy billet. The microstructure consists of primary  $\alpha$  phase (white particle in Fig.1) which is uniformly distributed in the transformed  $\beta$  matrix (black zone in Fig.1). The primary  $\alpha$  phase presents equiaxed morphology with a mean diameter of 1  $\mu\text{m}$ .

For a  $\beta$  titanium alloy,  $\alpha/\beta$  solution treatment leads to precipitations of primary  $\alpha$  phase in the  $\beta$  matrix. The shape and volume content of primary  $\alpha$  phases has obvious variance in different solution treated conditions. In order to approach the influence of primary  $\alpha$  phase morphology on the mechanical behavior, the alloy was solution treated below the  $\beta$  transus temperature. The heat treatment variables employed in the present work are shown in Table 1.

Microstructure characterizations were observed using the OLYMPUSPM-G3 optical microscope and SEM-JSM6460 scan electron microscope. The samples for OM/SEM observation were prepared by the conventional metallographic methods followed by etching in the Kroll's reagent (5% HF+15% HNO<sub>3</sub>+80% H<sub>2</sub>O)<sup>[14]</sup>.

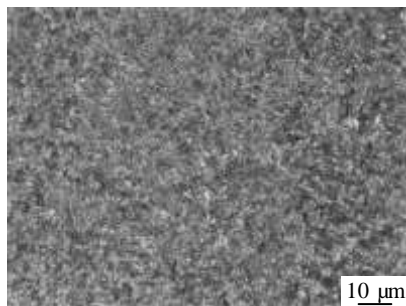


Fig.1 Original microstructure of alloy billet

**Table 1 Heat treatment processes employed in the present work**

Specimen No.	Solution	Aging
1	870 °C/1 h, AC	
2	870 °C/1 h, AC+850 °C/1 h, AC	
3	870 °C/1 h, FC(0.5 °C/min) to 850 °C/1 h, AC	620 °C/6 h, AC
4	870 °C/1 h, FC(0.5 °C/min) to 620 °C, AC	

Image analysis software was used to calculate the size of primary  $\alpha$  phase based on the micrographs. The tensile tests were carried out on the Instron 5985 testing machine. Fracture toughness tests were conducted using standard CT (compact tension) specimens with dimensions of 50 mm×48 mm×20 mm in accordance with ASTM standard E-399<sup>[15]</sup> by an MTS810 fatigue testing machine.

## 2 Results and Discussion

### 2.1 Morphology of primary $\alpha$ phase

The morphologies of specimens processed by different solution treatments are shown in Fig. 2. In Fig. 2a, spherical  $\alpha_p$  phase is made up of equiaxed structure and these small components have similar dimensions in each direction. Compared with other morphologies, its size is the smallest and the average diameter of equiaxed  $\alpha_p$  phase is approximately 0.5  $\mu\text{m}$ . Compared with specimen 1, the  $\alpha_p$  phases obtained in the specimen 2 exhibit a little larger globular shapes (Fig. 2b). It is supposed that the primary  $\alpha$  phases tend to globular growth on the basis of the equiaxed  $\alpha$  phases in the microstructure of specimen 1.

Fig.2c, 2d shows the microstructure of alloy treated by solution followed by furnace cooling. According to Fig.2c and 2d, abnormal growth of primary  $\alpha$  grains occurs in the furnace cooling process, and furnace cooling induces coarser grains in contrast to that followed by air cooling. It is apparent that except that some primary  $\alpha$  remains spherical growth, the other part evolves into similar dendritic growth rather than keeping nearly spherical growth trend. The microstructure of the specimen 3 consists of different morphologies: thin billet-like shape and polygon shape (Fig. 2c). The thin billet-like shape  $\alpha$  can later form thicker  $\alpha$  platelets with a small length-width ratio when the temperature of furnace cooling gets to  $620^\circ\text{C}$ , as can be seen in Fig.2d. In addition, the thicker lamellar  $\alpha$  tip is "fork" shaped morphology<sup>[16]</sup>.

From the microstructures of  $\alpha_p$  after furnace cooling process, it can be seen that growth of lamellar  $\alpha$  is usually more advantageous than that of equiaxed  $\alpha$ , and the growth rate of lamellar  $\alpha$  far exceeds the coarsening rate of equiaxed  $\alpha$ . Part of the reason is that nucleated and grown lamellar  $\alpha$  would hinder further coarsening of equiaxed  $\alpha$ . Another reason is that the growth rate of the lamellar tip is high<sup>[17]</sup>.

The effect of furnace cooling condition on evolution of microstructure has been studied systematically through measurements of different microstructural parameters such as  $\alpha$  length



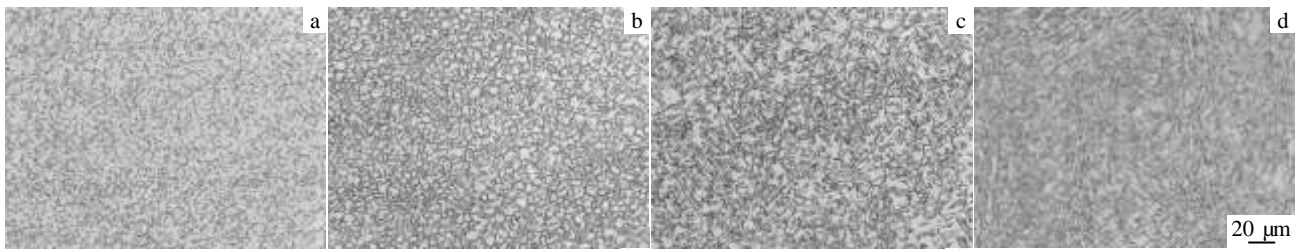


Fig.2 Morphologies of primary  $\alpha$  phase after different solution treatments: (a) specimen 1, (b) specimen 2, (c) specimen 3, and (d) specimen 4

and width. The morphology characteristics of the primary  $\alpha$  phase was described using equivalent diameter  $D$ , representing the size of the  $\alpha$  phase particles and shape factor  $Q$ , representing the spheroidizing degree<sup>[18]</sup>. The value of  $D$  is smaller and the  $Q$  value is close to 1 which shows that the particles are smaller, and spheroidizing degree is better. The values of  $D$  and  $Q$  under different solution treatment are shown in Fig. 3. It is observed that the  $Q$  value after single solution treatment (specimen 1) approaches to 1 and decreases with adding of specimen number, but the  $D$  value changes in the opposite way. That is to say the morphology of equiaxed  $\alpha$  phase can occur obviously change after continuous furnace cooling and the size of  $\alpha$  phase increases with the decreasing of furnace cooling temperature.

## 2.2 Mechanical properties

The tensile properties of the alloy with different primary  $\alpha$  morphologies are shown in Table 2. The alloy after single solution treatment at 870 °C followed by air cooling (specimen 1) has the highest ultimate strength with the lowest ductility. The tensile strength of the alloy after double solution treatment at 870 and 850 °C followed by air cooling (specimen 2) decreases from 990 MPa (specimen 1) to 970 MPa with the size of the primary  $\alpha$  phase grown up from 0.5  $\mu\text{m}$  to 1  $\mu\text{m}$ . Both the two solution treated samples share the same ductility values (~14% of elongation and ~50% of reduction of area). The decrease of the tensile strength is connected with the decline of the equiaxed  $\alpha$  phases size. The relationship between the strength and the size of  $\alpha$  phase accords with Hall-Petch mechanism<sup>[19]</sup>.

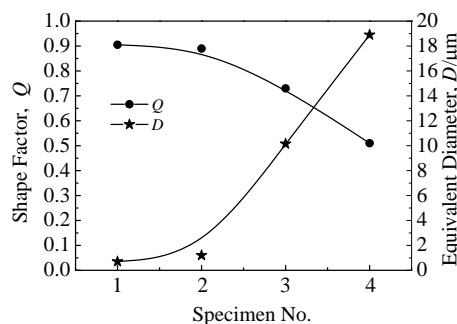


Fig.3 Value of shape factor  $Q$  and the equivalent diameter  $D$  of  $\alpha_p$  phase

Compared with air cooling, the tensile strength varies un-conspicuously after treated in the FC process, while the plasticity increases obviously. As a result, the alloy after solution treatment at 870 °C followed by furnace cooling to 620 °C (specimen 4) has a moderate strength level (950 MPa) with an excellent ductility (20.5% of elongation and 55% of reduction of area). It means that the tensile properties of the alloy after  $\alpha/\beta$  solution treatment are very sensitive to the morphologies of primary  $\alpha$ . The relatively higher strength after solution treatment by air cooling can be attributed to the fine-grain strengthening of equiaxed primary  $\alpha$ . It is easy for fine equiaxed primary  $\alpha$  to cause the dislocation piling up, leading to a higher tensile strength. But the reason why higher plasticity is attributed to thicker  $\alpha$  platelets with a small length-width ratio is not clear.

The tensile properties and fracture toughness of the alloys with all four solution treatment plus aging at 620 °C for 6 h air cooling are given in Table 3. According to Table 3, compared with the solution treated alloy, since substantial secondary  $\alpha$  phase occurs during aging, the strength of specimens 1, 2, 3 is significantly higher than that of solution treated alloys, but the ductility declines. The alloy is hardened to 1200 MPa of the ultimate strength with about 10% of elongation. By comparison, the tensile strength value of specimen 4 gets clearly lower than that of those of specimens 1, 2 and 3, which ultimate tensile strength is merely 1000 MPa with an excellent ductility

Table 2 Tensile properties of the specimens after different solution treatments

Specimen number	$R_m$ /MPa	$R_{p0.2}$ /MPa	$A$ /%	$Z$ /%
1	990	930	13.0	42.5
2	970	910	14.5	49.5
3	940	900	18.5	54
4	950	920	20.5	55

Table 3 Mechanical properties of the specimens after different solution treatments plus aging

Specimen number	$R_m$ /MPa	$R_{p0.2}$ /MPa	$A$ /%	$Z$ /%	$K_{IC}$ /MPa $\text{m}^{1/2}$
1	1310	1260	10.0	32.0	40.6
2	1280	1230	10.5	39.0	45.6
3	1300	1240	10.5	38.0	47.21
4	1000	930	19.0	42.0	87.9

(19% of elongation). Obviously, the first three kinds of heat treatment condition are more attractive.

But the fracture toughness exhibits a reverse trend to the strength. The fracture toughness of specimen 4 exhibits the largest values of about  $K_{IC}=87.9 \text{ MPa m}^{1/2}$ , while the fracture toughness of the alloy with tensile strength approaching 1300 MPa is  $40\sim 50 \text{ MPa m}^{1/2}$ . The reason of higher toughness of specimen 4 is that lamellar  $\alpha$  structure exhibits greater toughness compared with equiaxed  $\alpha$  structure, and coarsening of lamellar  $\alpha$  structure is very effective to achieve toughness in titanium alloys [20].

Fig.4 shows SEM microstructures of the alloy after different solution treatments plus aging. As seen in Fig.4a, 4b and 4c, the microstructure is composed of a mixture of pri-

mary  $\alpha$  ( $\alpha_p$ ), second  $\alpha$  ( $\alpha_s$ ) and  $\beta$  matrix. The dark  $\alpha_p$  phase with various shapes forms during solution treatment, and the  $\alpha_s$  phase with acicular shape of around 500~800 nm in length precipitates in  $\beta$  matrix during aging. To the contrary, in the microstructure of the specimen 4 the secondary  $\alpha$  phase is hardly observed, as can be seen in Fig.4d. A possible explanation for this is that remnant  $\beta$  could not provide a high enough driving force for the nucleation of  $\alpha_s$  phase during aging when the volume fraction of  $\alpha_p$  phase exceeds 60%.

Fig.5 shows SEM fractographs of the alloy with various heat treatments. Through the analysis on SEM images of the fracture specimen, it is found that the specimens are typical ductile intergranular fracture. By comparison, there are larger and deeper dimples in specimen 4 than that in specimen 1.

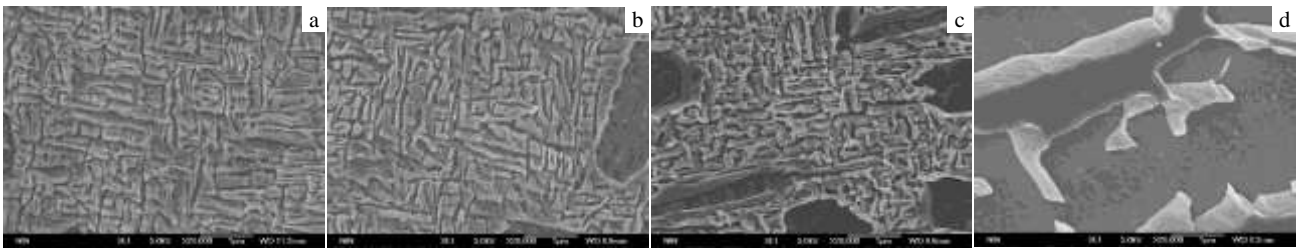


Fig.4 Microstructures of the alloy after solution treatment plus aging: (a) specimen 1, (b) specimen 2, (c) specimen 3, and (d) specimen 4

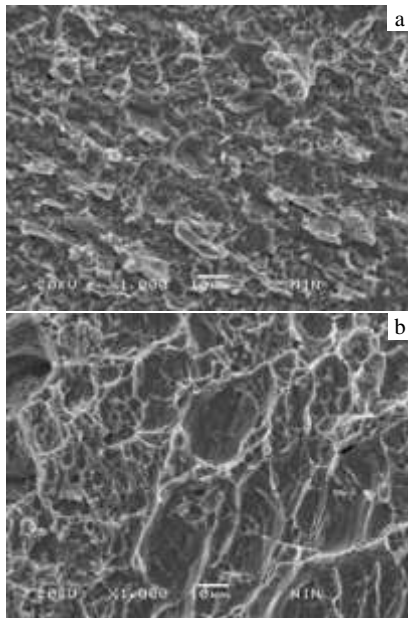


Fig.5 SEM images of fracture surfaces of specimen 1 (a) and specimen 4 (b)

### 3 Conclusions

1) Primary  $\alpha$  phases exhibit a globular growth feature on the basis of the equiaxed  $\alpha$  phases after double solution treatment

at air cooling of  $\alpha/\beta$  zone. But abnormal growth of primary  $\alpha$  grains occurs in the  $0.5^\circ\text{C}/\text{min}$  furnace cooling process except that some primary  $\alpha$  remains spherical growth. The other part evolve into similar “fork” shaped dendritic growth rather than keeping nearly spherical growth trend.

2) Microstructures obtain a few equiaxed or thin billet-like primary  $\alpha$  phase and fine lamellar secondary  $\alpha$  phase under  $\alpha/\beta$  solution treatment followed by air cooling plus aging, which leads to attractive combinations of strength and ductility ( $\approx 1300 \text{ MPa}$  of ultimate strength with 10.5% of elongation). Compared with other high strength titanium alloys (Ti-5553, Ti-1023, VT22, etc.), the new type titanium alloy has giant competitiveness.

3) After  $\alpha/\beta$  solution treatment followed by  $0.5^\circ\text{C}/\text{min}$  furnace cooling to low temperature and then aging heat treatment process, the alloy exhibits an excellent fracture toughness ( $\geq 80 \text{ MPa m}^{1/2}$ ). Meanwhile, the elongation and reduction of area remain at about 19% and 42%, respectively, and its corresponding tensile strength maintains at about 1000 MPa. It can be assumed that the alloy may be a usable structural material.

### References

- 1 Ahmed Mansur, Savvakina G Dmytro, Ivasishin M Orest et al. *Materials Science and Engineering A*[J], 2013, 576: 167
- 2 Song Zhenya, Sun Qiaoyan, Xiao Lin et al. *Rare Metal Materials and Engineering*[J], 2014, 43(7): 1543

- 3 Zhang Yaowu, Kent Damon, Wang Gui et al. *Journal of the Mechanical Behavior of Biomedical Materials*[J], 2015, 42: 207
- 4 Chen Yuyong, Du Zhaoxin, Xiao Shulong et al. *Journal of Alloys and Compounds*[J], 2014, 586: 588
- 5 Huang Liguang, Chen Yuyong. *Materials and Design*[J], 2015, 66: 110
- 6 Chen Jun, Chang Hui, Li Hui. *Acta Metall Sin*[J], 2002, 38: 108
- 7 Guo Ping, Zhao Yongqing, Zeng Weidong. *Rare Metal Materials and Engineering*[J], 2015, 44(2): 277
- 8 Du Zhaoxin, Xiao Shulong, Xu Lijuan et al. *Materials and Design*[J], 2014, 55: 183
- 9 Ghosh Atasi, Sivaprasad S, Bhattacharjee Amit et al. *Materials Science and Engineering A*[J], 2013, 568: 61
- 10 Wain N, Hao X J, RaviG A et al. *Materials Science and Engineering A*[J], 2010, 527: 7673
- 11 Li Chenglin, Mi Xujun, Ye Wenjun et al. *Materials Science and Engineering A*[J], 2013, 578: 103
- 12 Ibrahim Khaled M, Mhaede Mansour, Wagner Lothar. *Trans Nonferrous Met Soc China* [J], 2012, 22: 2609
- 13 Li Chenglin, Mi Xujun, Ye Wenjun et al. *Journal of Alloys and Compounds*[J], 2013, 550: 23
- 14 Li Chenglin, Mi Xujun, Ye Wenjun et al. *Materials Science and Engineering A* [J], 2013, 580: 250
- 15 Paradkar Archana, Kumar Vikas, Kamat S V et al. *Materials Science and Engineering A* [J], 2008, 486: 273
- 16 KartikPrasad, RajdeepSarkar, Kamat S V et al. *Materials Science and Engineering A*[J], 2011, 529: 74
- 17 Sun Zhichao, Guo Shuangshuang, Yang He. *Acta Materialia*[J], 2013, 61: 2057
- 18 Wang K, Li M Q. *Materials Science and Engineering A*[J], 2014, 613: 209
- 19 Li Huabing, Jiang Zhouhua, Zhang Zurui et al. *Journal of Iron and Steel Research* [J], 2009, 1: 58
- 20 Niinomi M, Kobayashi T. *Materials Science and Engineering A*[J], 1996, 213: 16

## 一种新型高强钛合金热处理过程中初生相形态演变和力学性能

周 伟, 葛 鹏, 赵永庆, 辛社伟, 李 倩, 陈 军, 张思远, 黄朝文

(西北有色金属研究院, 陕西 西安 710016)

**摘 要:** 对一种新型高强  $\beta$  钛合金热处理过程中初生  $\alpha$  相形貌演变和力学性能进行了研究。结果表明: 新型合金  $\alpha/\beta$  区双重固溶处理时初生  $\alpha$  相在原有近球形晶粒基础上呈现球状生长; 固溶后以  $0.5\text{ }^{\circ}\text{C}/\text{min}$  冷却速率炉冷, 除部分初生  $\alpha$  相依然保持近球状生长外, 另有部分  $\alpha$  相出现了  $\alpha$  相端面的“叉型”结构定向生长特征。新型合金  $\alpha/\beta$  区固溶后空冷+时效处理获得的细小等轴或短棒状初生  $\alpha$  相与针状次生  $\alpha$  相的混合组织具有优异的强-塑性匹配(抗拉强度 1300 MPa, 延伸率 10.5%)。固溶后炉冷+时效处理的合金的抗拉强度为 1000 MPa, 延伸率为 19%, 断面收缩率为 45%, 且具有优异的断裂韧性 ( $\geq 80\text{ MPa m}^{1/2}$ )。认为该合金是一种优良的结构材料。

**关键词:** 热处理; 钛合金; 初生 $\alpha$ 相; 力学性能

---

作者简介: 周 伟, 女, 1978 年生, 硕士, 西北有色金属研究院钛合金研究所, 陕西 西安 710016, 电话: 029-86250729, E-mail: zhouwei2002563@163.com